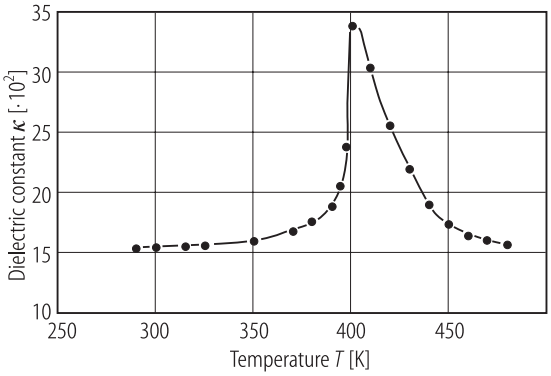

Fig. 1A-10-060. $BaTiO_3$ (thin film). κ vs. T [93Des]. f = 1 MHz. Film thickness: 220 nm. Substrate: Si single crystal. Deposition temperature: 650 °C. Deposition pressure: 2 Pa.

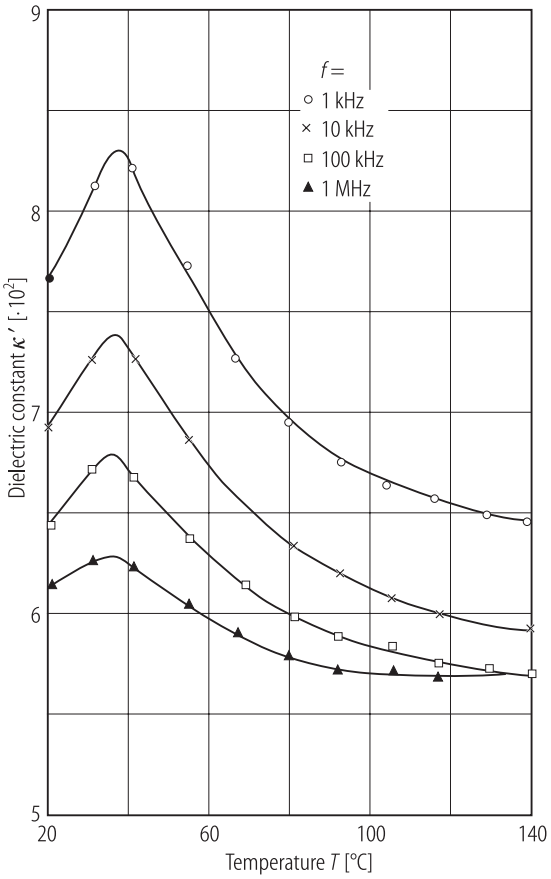

Fig. 1A-10-061. $BaTiO_3$ (thin film). κ' vs. T [93Kam]. Parameter: f. The thin film was grown by sol-gel method on the platinum substrate. Film thickness: 2.5 μm.

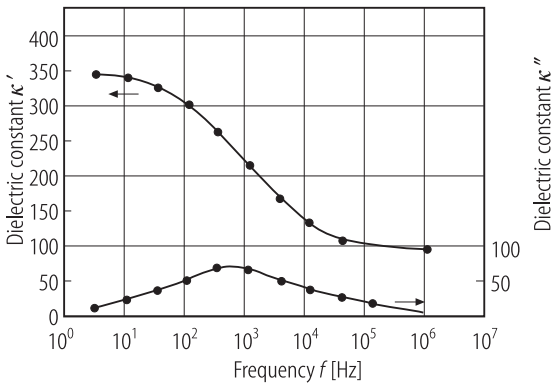

Fig. 1A-10-062. $BaTiO_3$ (thin film). κ', κ'' vs. f [93Kam]. The thin film was grown by sol-gel method on stainless-steel plate. Film thickness: 1 μm.

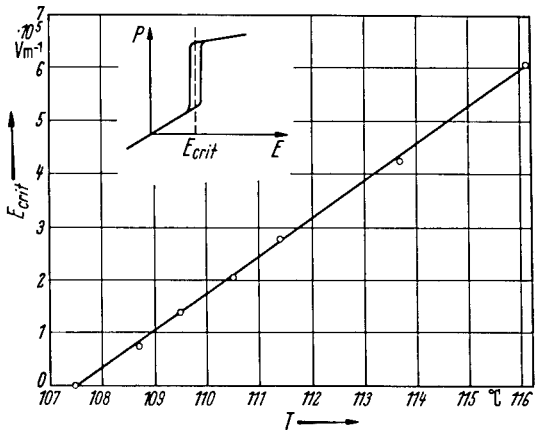

Fig. 1A-10-063. $BaTiO_3$. E_{crit} vs. T [53Mer]. E_{crit}: electric field strength associated with the induced P–F phase transition above the Curie temperature. For definition, see the insert.

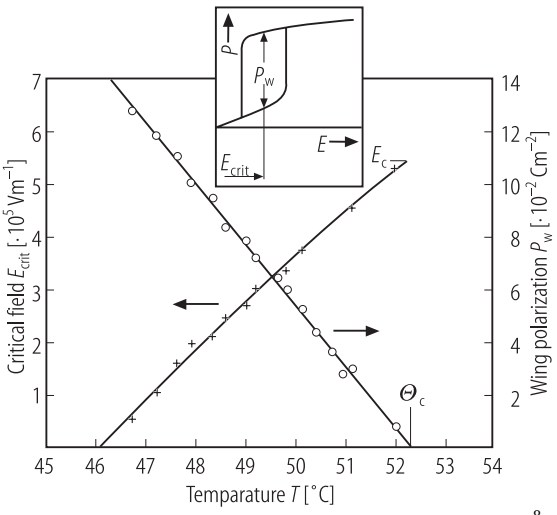

Fig. 1A-10-064. $BaTiO_3$. E_{crit}, P_w vs. T at $13.3 \cdot 10^8$ Pa [89Dec]. E_{crit}: electric field strength associated with the induced P–F phase transition. P_w: wing polarization. For definition, see the insert. (E_c, Θ_c): critical point in the E–T plane.

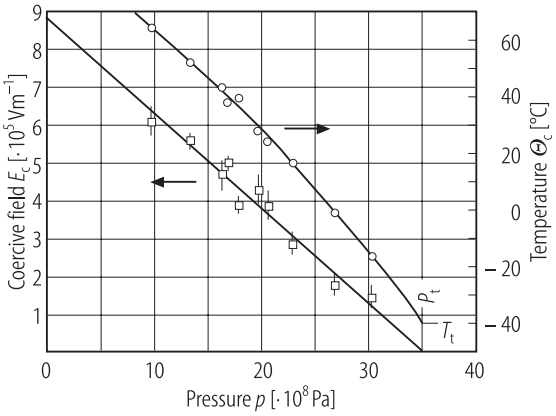

Fig. 1A-10-065. $BaTiO_3$. E_c, Θ_c vs. p [89Dec]. (E_c, Θ_c): critical point in the E–T plane. (P_t, T_t): (p, T) of tricritical point.

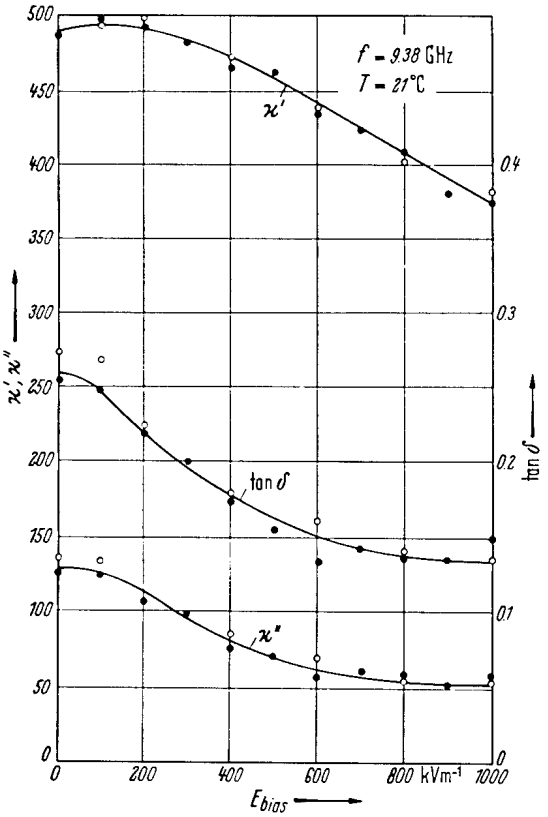

Fig. 1A-10-066. $BaTiO_3$ (ceramics). κ', κ'', $\tan\delta$ vs. E_{bias} [62Pop]. f = 9.38 GHz. T = 21 °C.

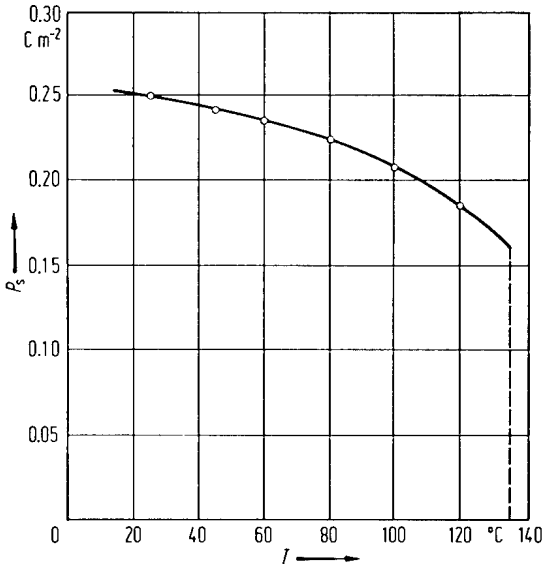

Fig. 1A-10-067. $BaTiO_3$. P_s vs. T [68Wem].

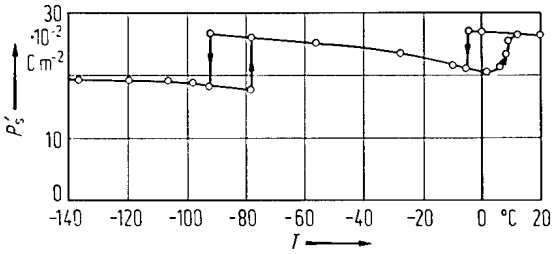

Fig. 1A-10-068. $BaTiO_3$. P'_s vs. T below RT [55Wie1]. P'_s: $P'_s = P_s$ in the phase II, and component of P_s along the pseudotetragonal [001] in the phase III.

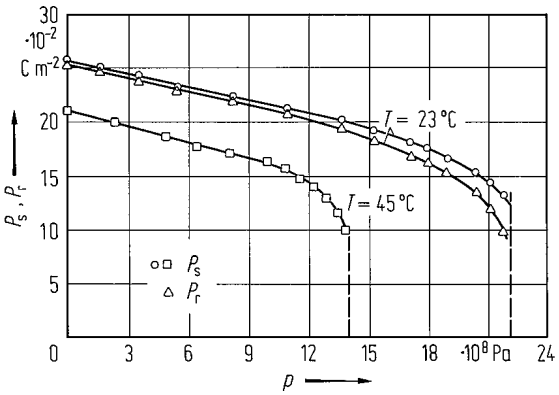

Fig. 1A-10-069. $BaTiO_3$. P_s, P_r vs. p at 23 °C and 45 °C [66Sam]. P_r: remanent polarization.

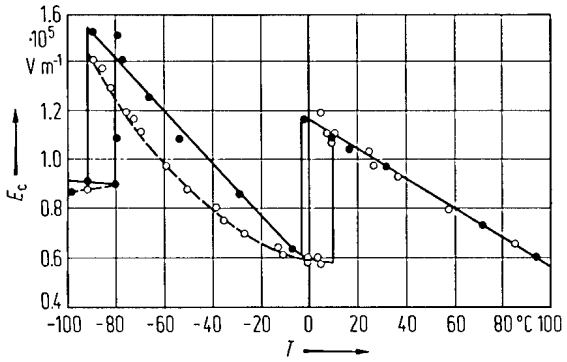

Fig. 1A-10-070. $BaTiO_3$. E_c vs. T [55Wie2]. Solid curve: *c*-domain crystal at 25 °C. Dashed curve: *c*-domain crystal having a number of *a*-domain wedges at 25 °C. E_c was measured with plates cut perpendicularly to the pseudocubic [001].

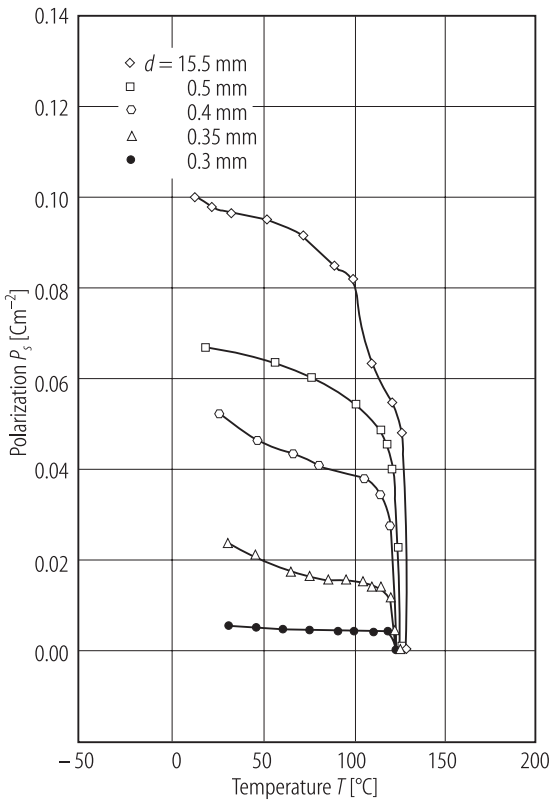

Fig. 1A-10-071. $BaTiO_3$ (ceramics). P_s vs. T [86Sha]. Parameter: d, average grain size.

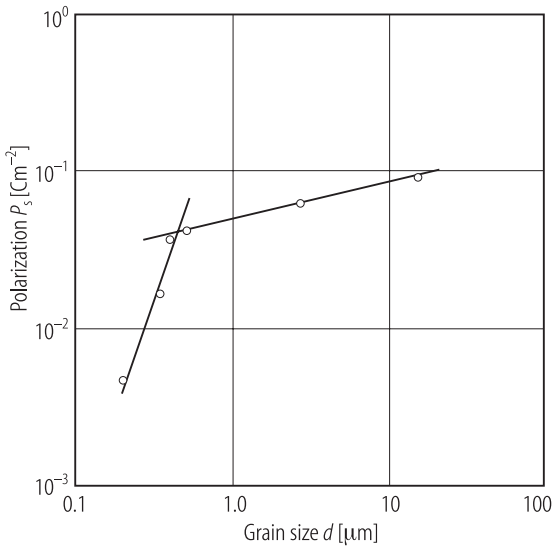

Fig. 1A-10-072. $BaTiO_3$ (ceramics). P_s vs. d at 70 °C [89Sha]. d: average grain size.

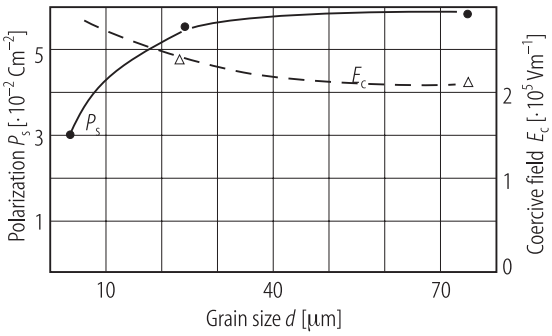

Fig. 1A-10-073. $BaTiO_3$ (ceramics). P_s, E_c vs. d [81Dam].
d: thickness of the specimens. T = RT.

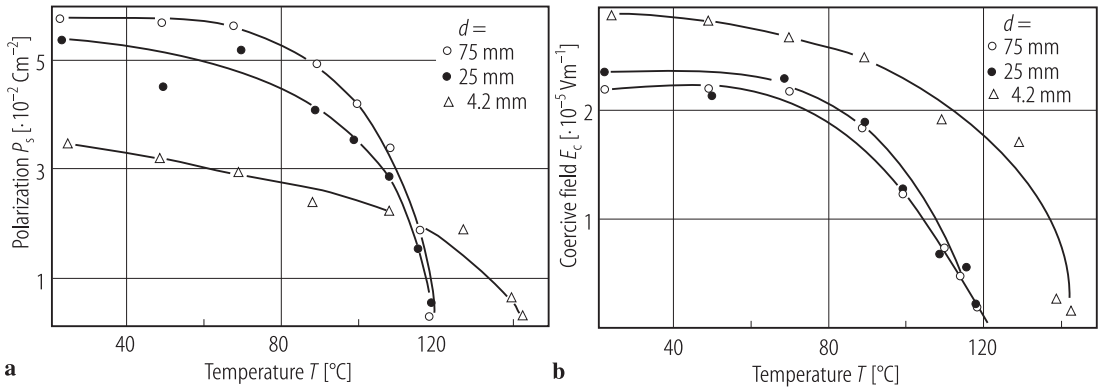

Fig. 1A-10-074. $BaTiO_3$ (ceramics). P_s (**a**), E_c (**b**) vs. T [81Dam]. Parameter: d, thickness of the specimens.

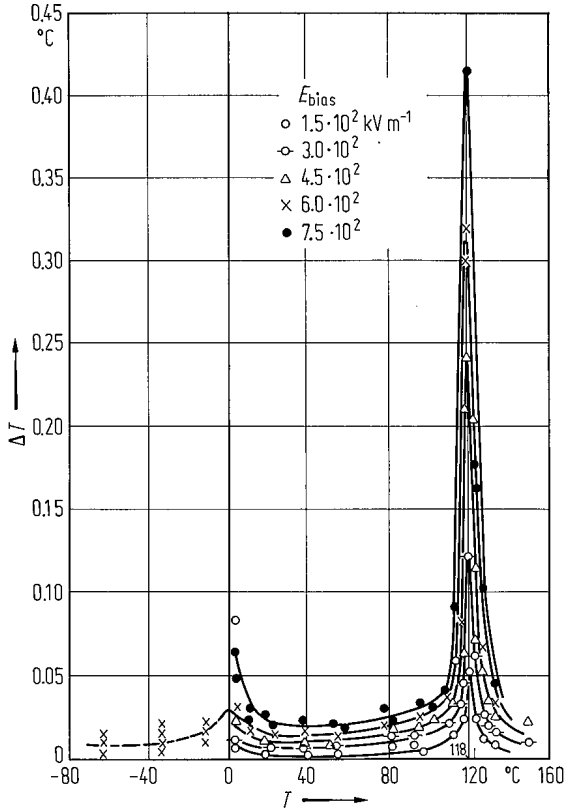

Fig. 1A-10-075. $BaTiO_3$ (ceramics). ΔT vs. T [61Kar]. Parameter: E_{bias}. ΔT: electrocaloric temperature change.

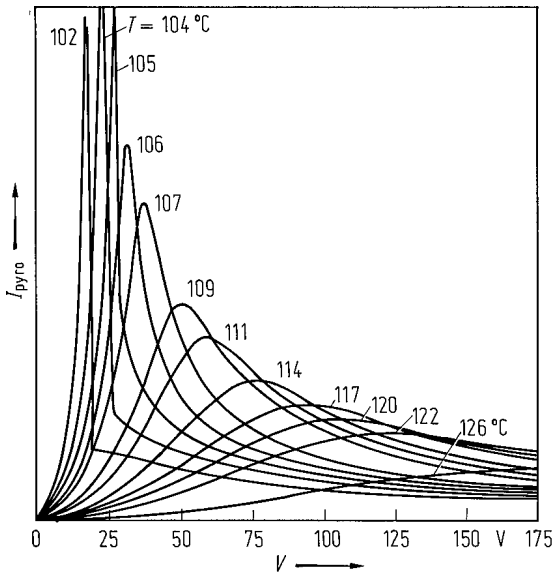

Fig. 1A-10-076. $BaTiO_3$. I_{pyro} vs. V [56Chy1]. Parameter: T. I_{pyro}: pyroelectric current measured by the dynamic method.

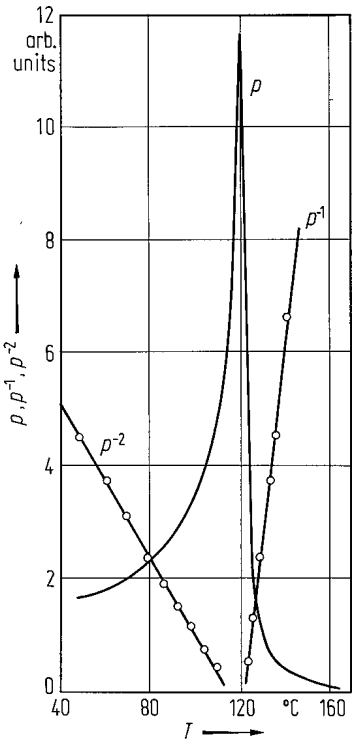

Fig. 1A-10-077. $BaTiO_3$ (ceramics). p, p^{-1}, p^{-2} vs. T [77Toy]. p: pyroelectric coefficient.

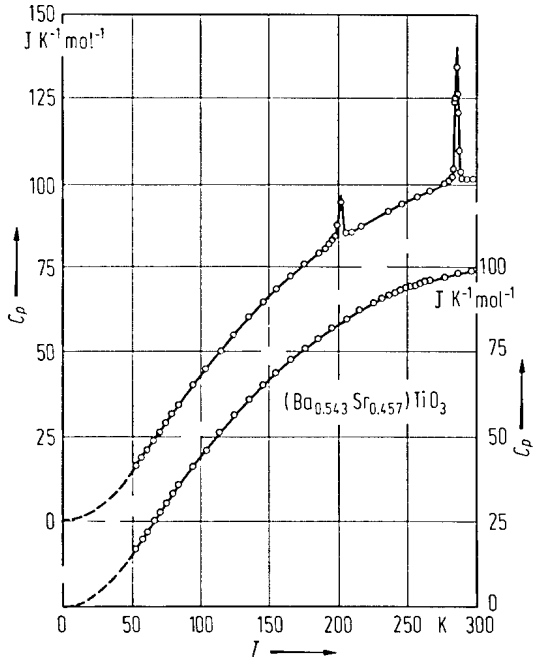

Fig. 1A-10-078. $BaTiO_3$ (ceramics). $Ba_{1-x}Sr_xTiO_3$. C_p vs. T [52Tod]. C_p: molar heat capacity at constant pressure.

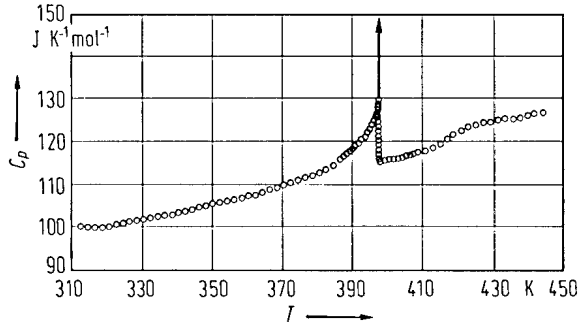

Fig. 1A-10-079. $BaTiO_3$. C_p vs. T [76Hat]. C_p: molar heat capacity at constant pressure.

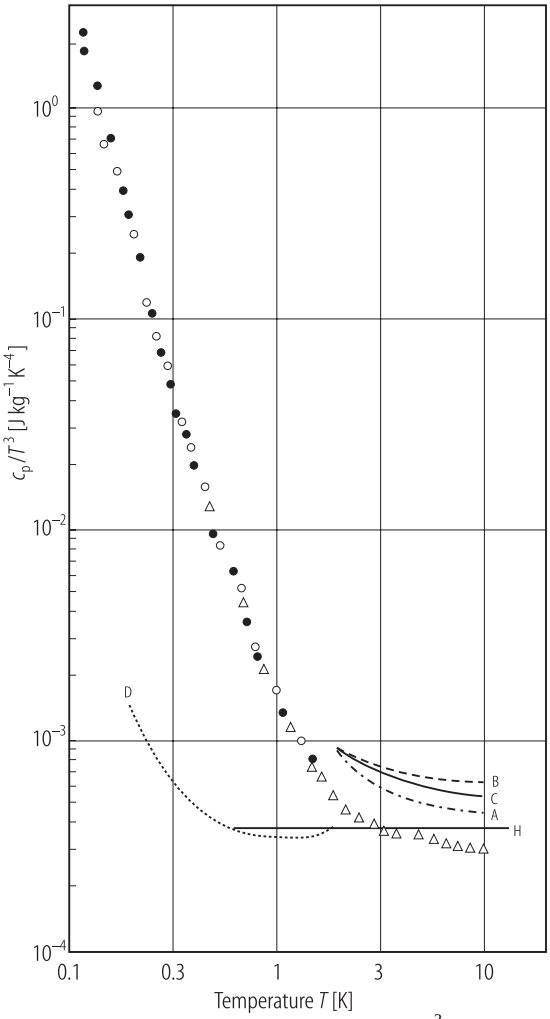

Fig. 1A-10-080. $BaTiO_3$ (ceramics). c_p/T^3 vs. T below 10 K [86Zim]. c_p: specific heat capacity at constant pressure. Circles, open triangles : present data of ceramics. A: poled ceramics [77Law]. B: unpoled ceramics [77Law]. C: single crystal [77Law]. D: single crystal [85Foo]. H: calculated results of Debye-contribution [78Law].

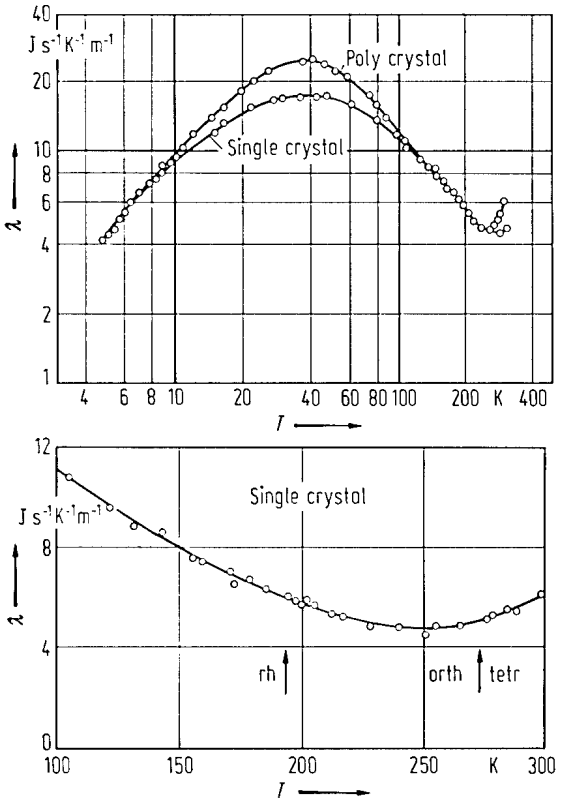

Fig. 1A-10-081. $BaTiO_3$. λ vs. T [65Sue]. λ: thermal conductivity.

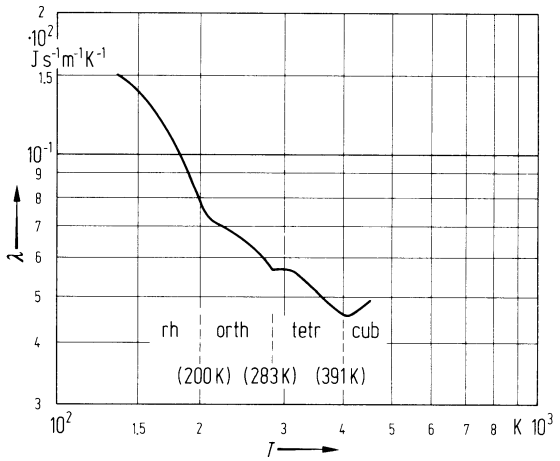

Fig. 1A-10-082. $BaTiO_3$. λ vs. T [67Man]. λ: thermal conductivity.

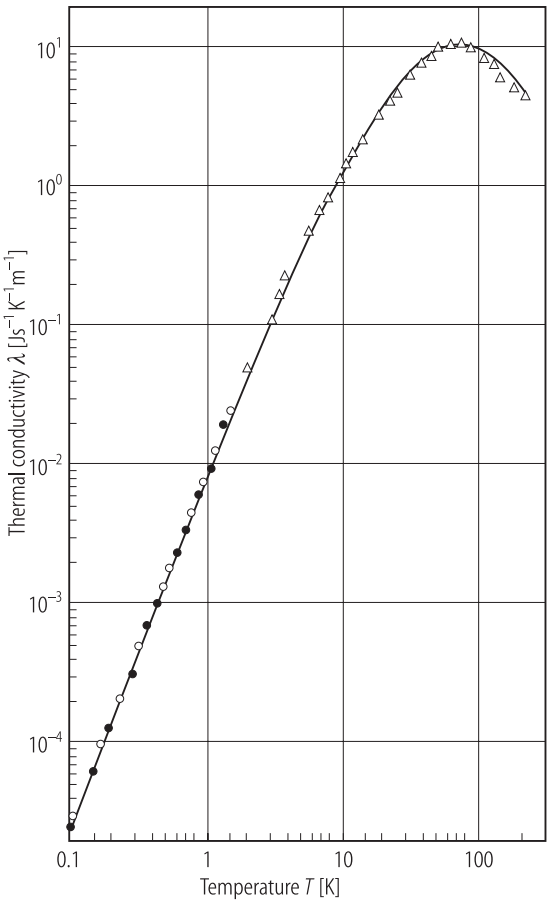

Fig. 1A-10-083. $BaTiO_3$ (ceramics). λ vs. T [86Zim]. λ: thermal conductivity. Open circles: unpolarized. Full circles: polarized. Open triangles: without any treatments.

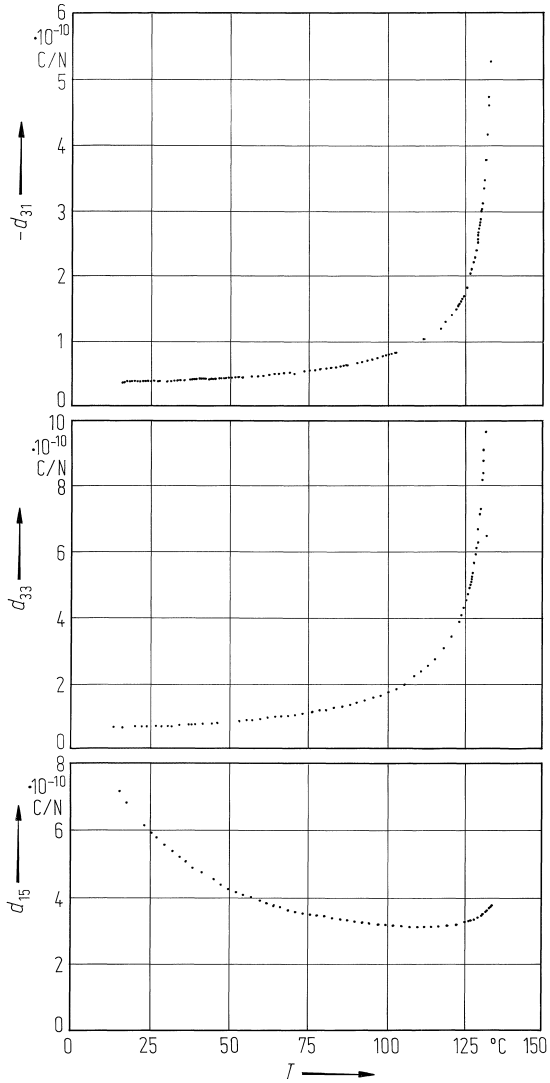

Fig. 1A-10-084. $BaTiO_3$. $d_{i\lambda}$ vs. T [86Sch]. The crystal was grown by top-seeded solution method.

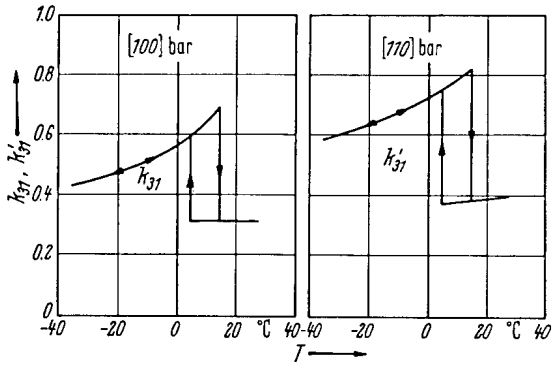

Fig. 1A-10-085. $BaTiO_3$. k_{31}, k'_{31} for [100] and [110] bars vs. T [58Ber].

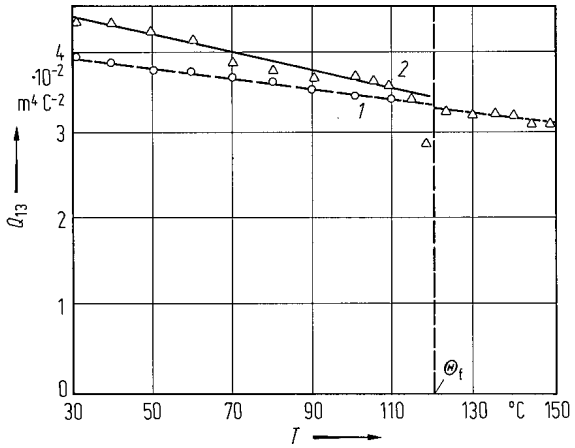

Fig. 1A-10-086. $BaTiO_3$. Q_{13} vs. T [59Hui]. Q_{13}: electrostrictive constant. Dashed line *1*: calculated from S_1/P_3^2 (S_1: determined from X-ray, P_3: determined from hysteresis loops). Solid line *2*: calculated from $g_{31}/(2P_3)$.

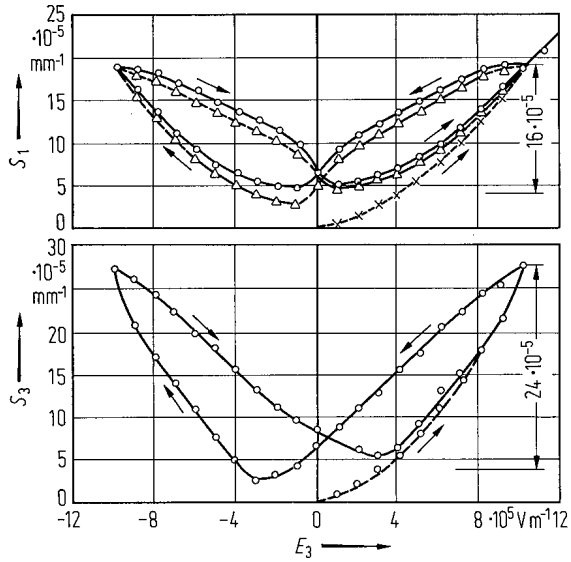

Fig. 1A-10-087. $BaTiO_3$ (ceramics). S_1, S_3 vs. E_3 [57Tak].
S_1: transverse strain. S_3: longitudinal strain.

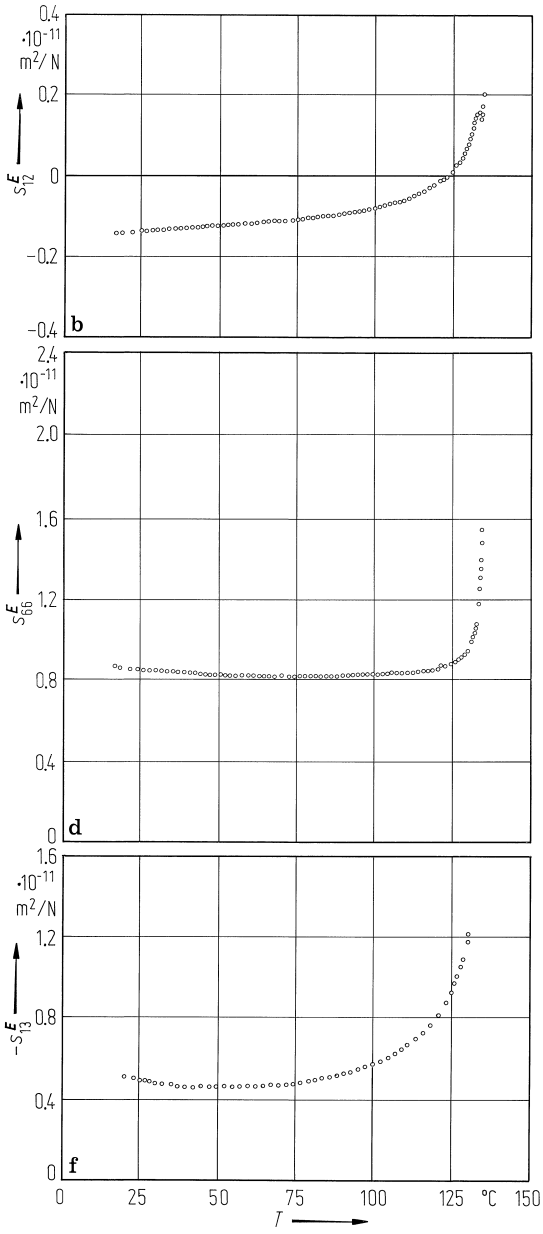

Fig. 1A-10-088. $BaTiO_3$. $s^E_{\lambda\mu}$ vs. T [86Sch]. The crystal was grown by top-seeded solution method.

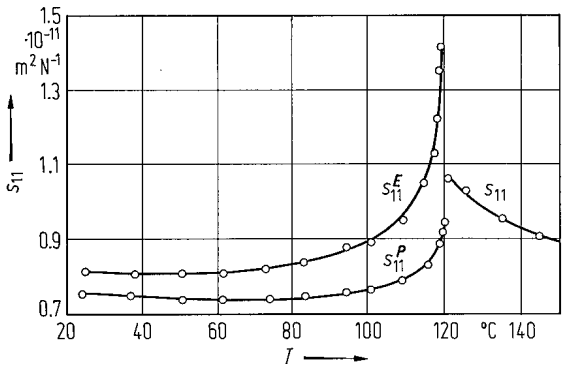

Fig. 1A-10-089. $BaTiO_3$. s_{11} vs. T [59Hui].

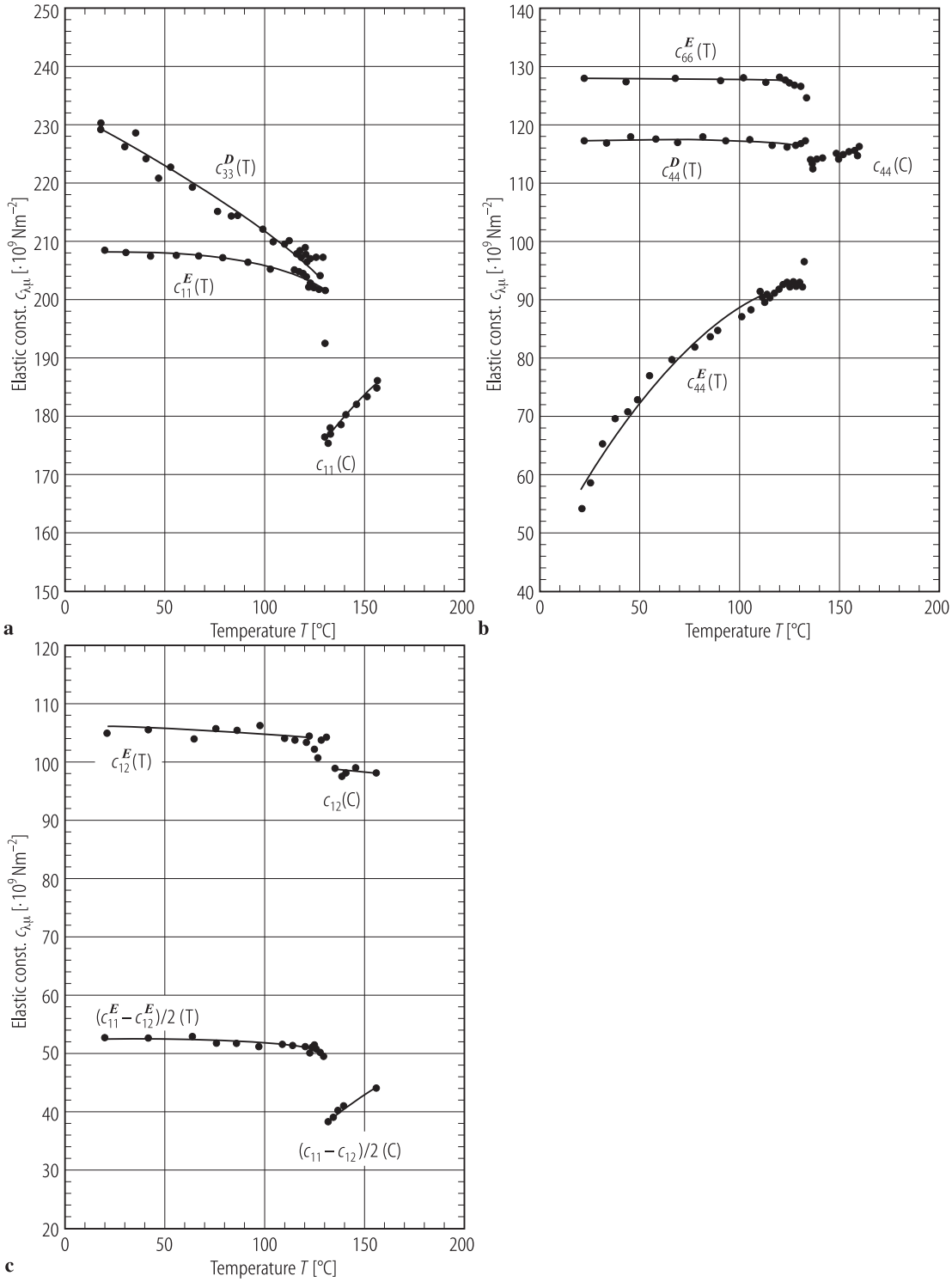

Fig. 1A-10-090. $BaTiO_3$. $c_{\lambda\mu}$ vs. T [94LiZ]. **(a)** c_{11}, c_{33}. **(b)** c_{44}, c_{66}. **(c)** c_{11}, c_{12}.

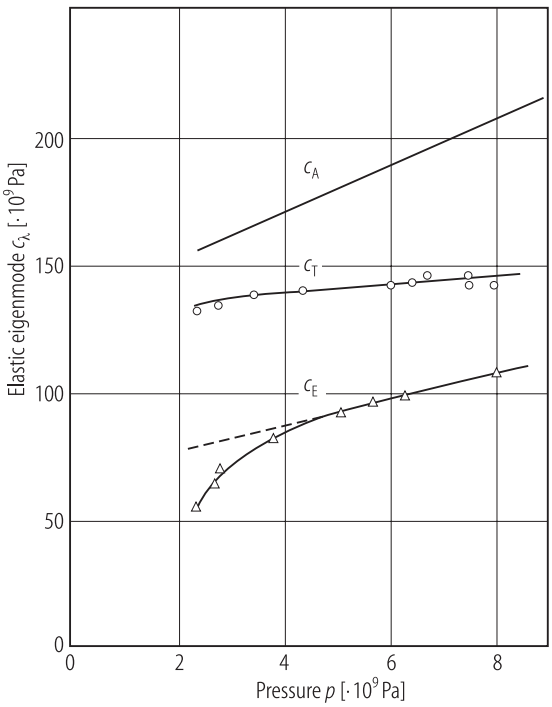

Fig. 1A-10-091. $BaTiO_3$. c_λ vs. p [89Ish]. c_λ: elastic eigenmode in the cubic phase. $c_A = (c_{11} + 2c_{12})/3$. $c_E = (c_{11} - c_{12})/2$. $c_T = c_{44}$. c_A was evaluated from observed c_{11} and c_E.

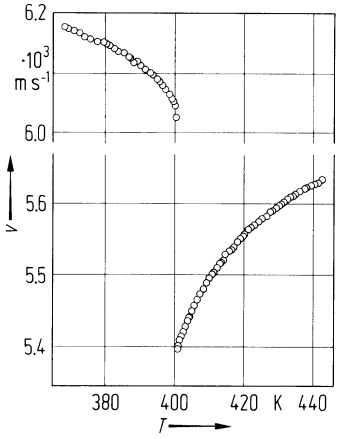

Fig. 1A-10-092. $BaTiO_3$. υ vs. T [73Kas]. υ : longitudinal sound velocity along [100] direction measured at 45 MHz.

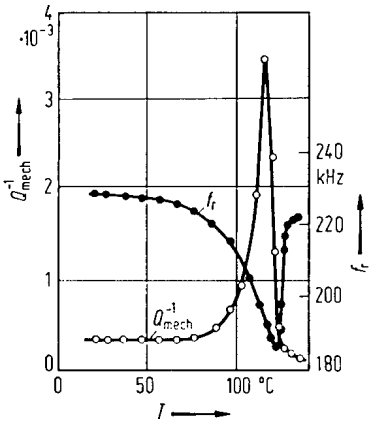

Fig. 1A-10-093. $BaTiO_3$. f_r, Q^{-1}_{mech} vs. T [69Kud]. f_r: resonance frequency of the crystal along [100].

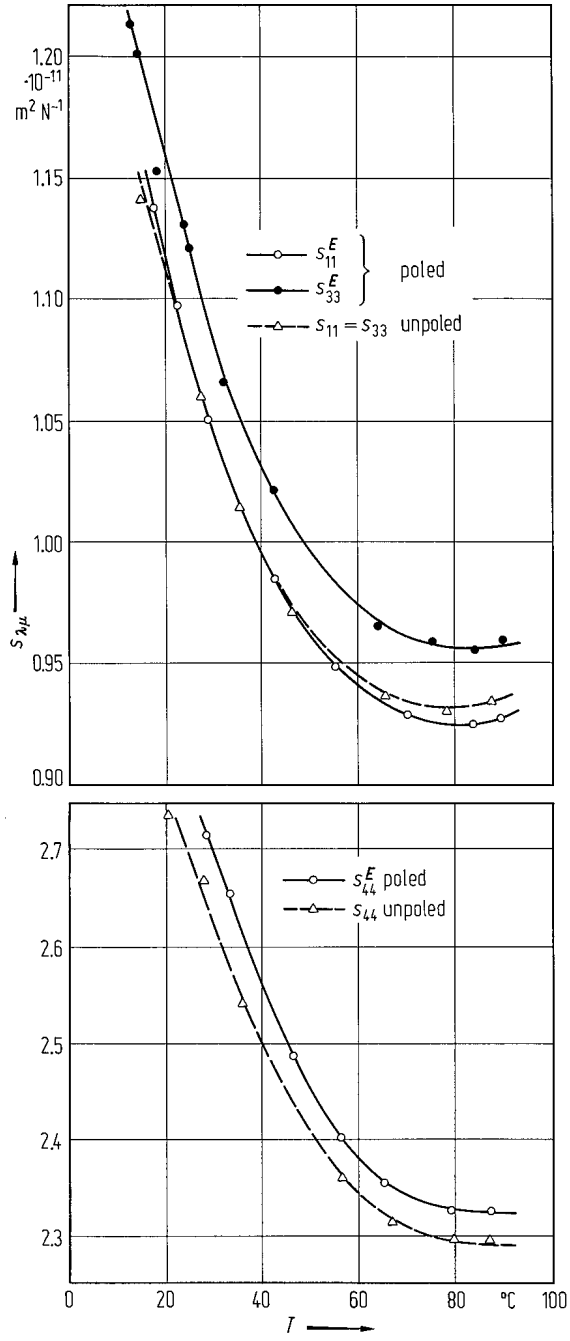

Fig. 1A-10-094. $BaTiO_3$ (ceramics). s_{11}, s_{33} (poled and unpoled specimens), s_{44} (unpoled specimen), s_{44}^E (poled specimen) vs. T [57Mar].

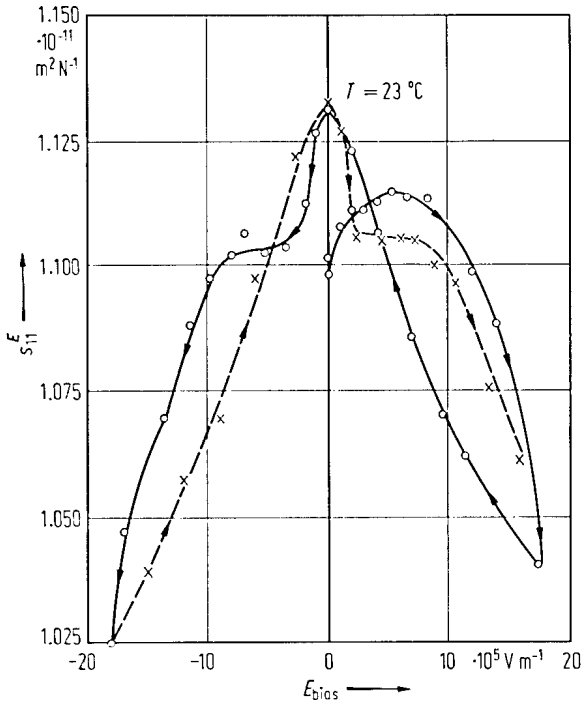

Fig. 1A-10-095. $BaTiO_3$ (ceramics). s_{11}^{E} vs. E_{bias} [57Mar].

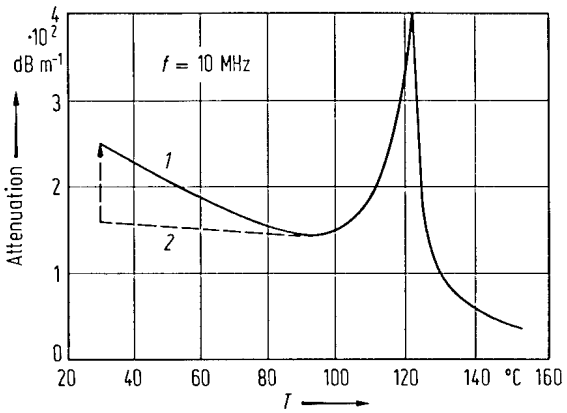

Fig. 1A-10-096. $BaTiO_3$ (ceramics). Attenuation vs. *T* [55Hue]. Pulse method. Curve *1*: unpoled sample, heating or cooling without bias. *2*: poled sample, cooling under bias.

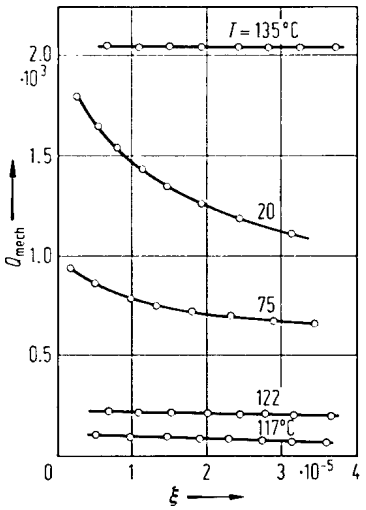

Fig. 1A-10-097. $BaTiO_3$. Q_{mech} vs. ξ [71Kud]. Parameter: *T*. ξ: deformation amplitude.

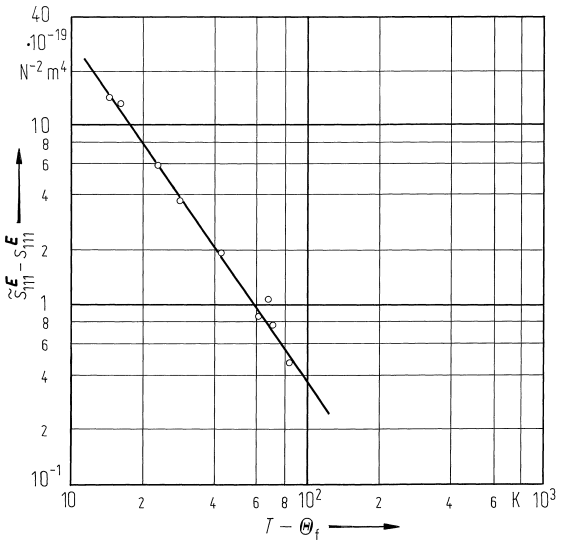

Fig. 1A-10-098. $BaTiO_3$. $\tilde{s}^E_{111} - s^E_{111}$ vs. $T - \Theta_f$ [80Bei]. $\tilde{s}^E_{111} - s^E_{111}$: anomalous part of the nonlinear elastic compliance.

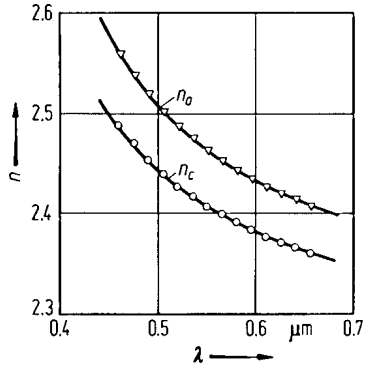

Fig. 1A-10-099. $BaTiO_3$. n_a and n_c vs. λ at RT [71Joh]. For the crystal grown by the top-seeded solution growth method, see [68Wem]. For the crystal grown by the TiO_2 rich melt, see [93Bus] and Table 1A-10-018.

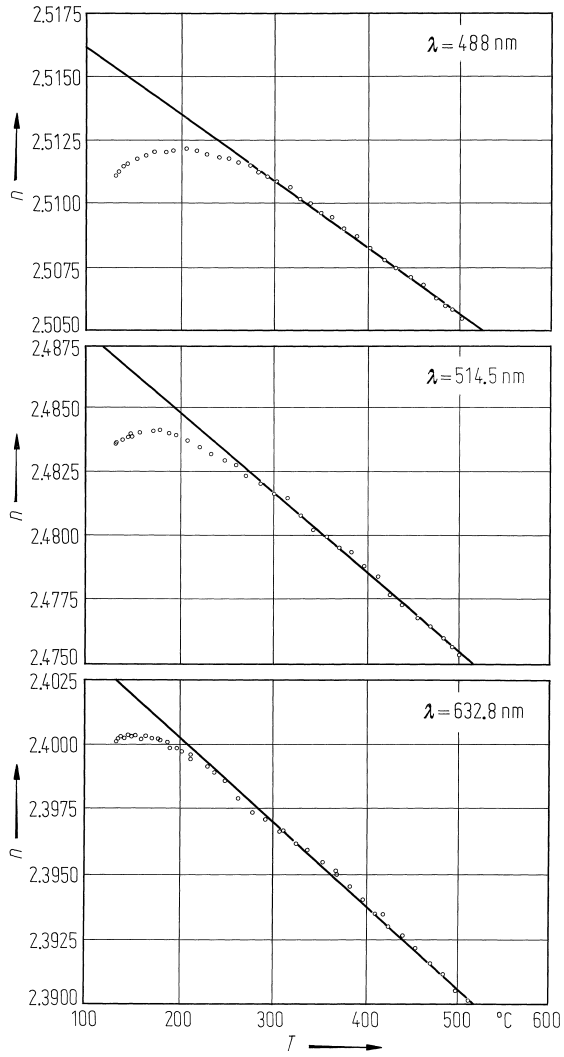

Fig. 1A-10-100. $BaTiO_3$. n vs. T [81Bur]. Parameter: λ, wavelength. The crystal was grown by the TiO_2 rich melt. For the flux grown crystal, see [82Bur]. For the crystals with additives of Fe, Mn, or Sr, see [90Bur].

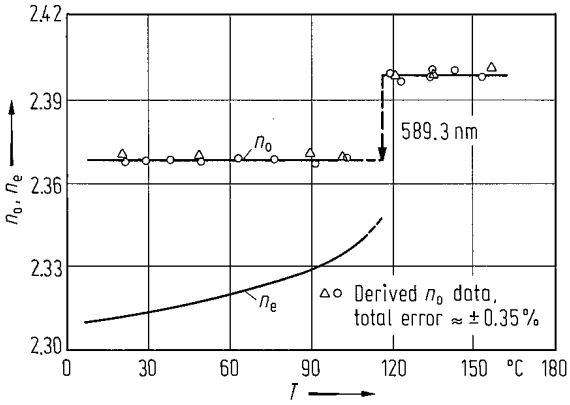

Fig. 1A-10-101. $BaTiO_3$. n vs. T [64Law]. λ = 589.3 nm.

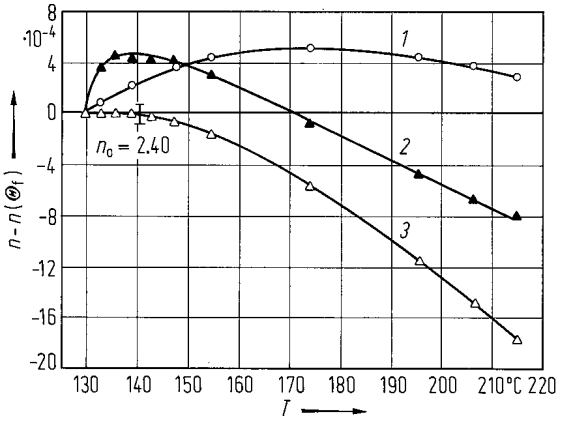

Fig. 1A-10-102. $BaTiO_3$. $n - n(\Theta_f)$ vs. T [65Bal]. $n(\Theta_f)$: n at Θ_f. λ = 632.8 nm. Curve *1*: uncorrected, *2*: corrected for thermal expansion with data of [47Meg], *3*: corrected for thermal expansion with data of [52Shi].

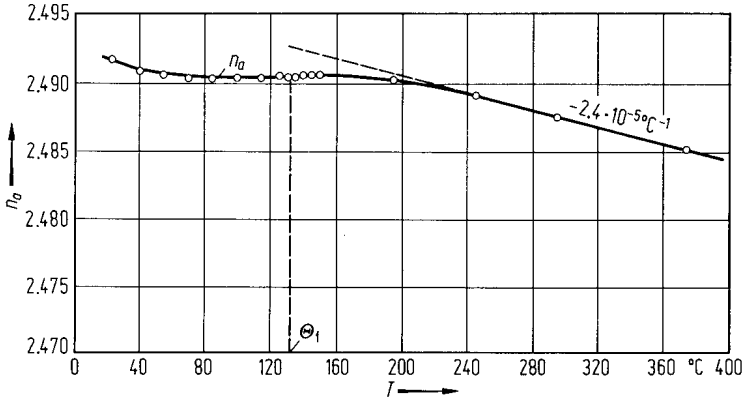

Fig. 1A-10-103. $BaTiO_3$. n_a vs. T [70Wem]. λ = 514.5 nm. The crystal was grown by the top-seeded solution technique.

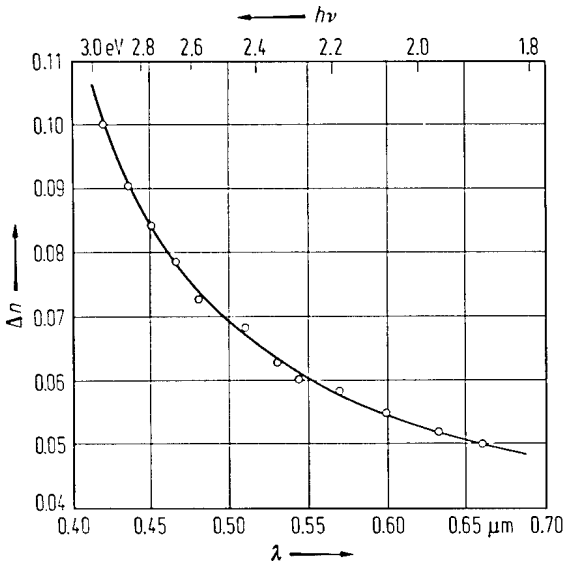

Fig. 1A-10-104. $BaTiO_3$. Δn vs. λ [68Wem]. T = 25 °C. The crystal was grown by the top-seeded solution technique; see also [86Rup] and [93Bus]. For the flux grown crystal, see [71Joh].

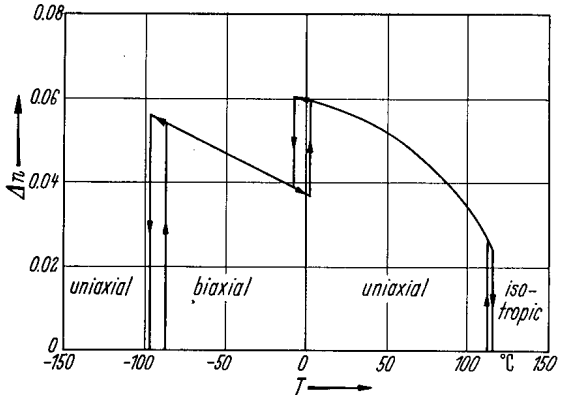

Fig. 1A-10-105. $BaTiO_3$. Δn vs. T [49Kay]. $\Delta n = n_a - n_c$. For green Hg line, see [58Mey]. For NaD line, see [49For]. For the crystal grown by the top-seeded solution technique, see [68Wem]. See also [88Kov].

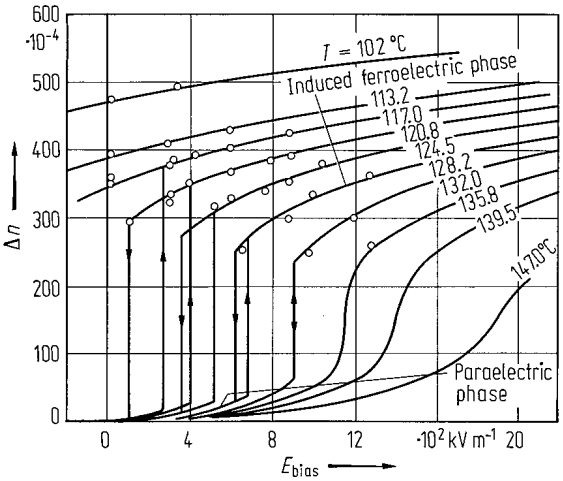

Fig. 1A-10-106. $BaTiO_3$. Δn vs. E_{bias} [58Mey]. $\Delta n = n_a - n_c$. Parameter: T. See also [66Per]. λ = 545 nm.

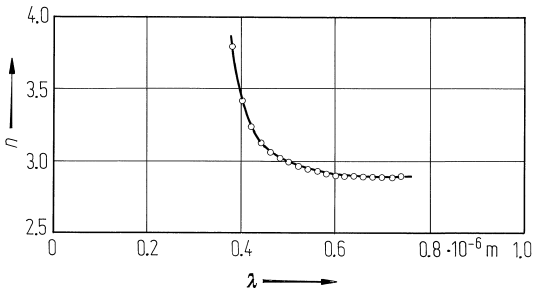

Fig. 1A-10-107. $BaTiO_3$ (thin film). n vs. λ [81Nag].

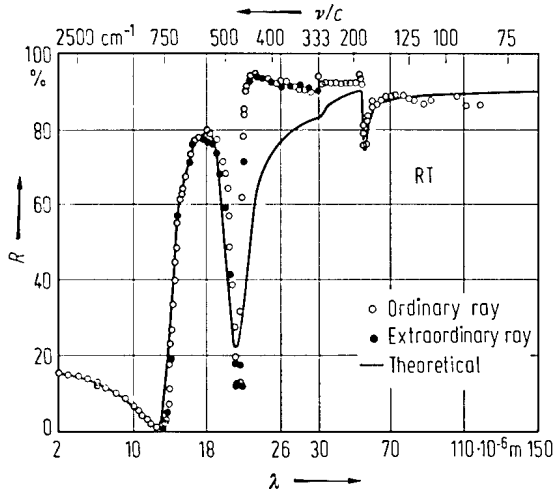

Fig. 1A-10-108. $BaTiO_3$. R vs. λ [62Spi]. R: reflectivity. See also [62Ike]. Note change of scale at $\lambda = 30 \cdot 10^{-6}$ m. The solid curve was calculated by using dispersion theory.

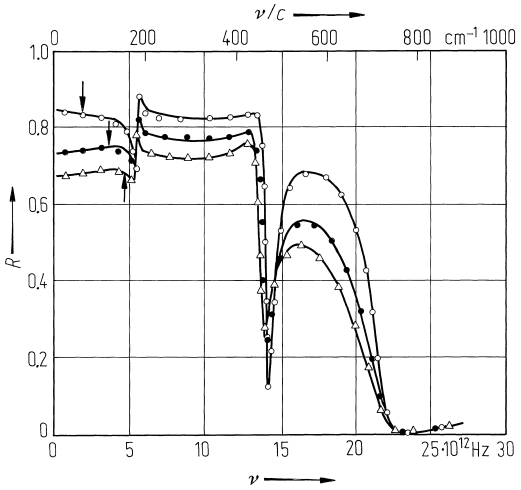

Fig. 1A-10-109. $BaTiO_3$. *R* vs. *ν* [80Lus]. Parameter: *T*. *R:* reflectivity of F_{1u}-type modes. *ν*: frequency. Open circles: 400 K. Full circles: 850 K. Open triangles: 1150 K. The curves are best fit of the dielectric function model to the data. The arrows indicate the soft mode frequency.

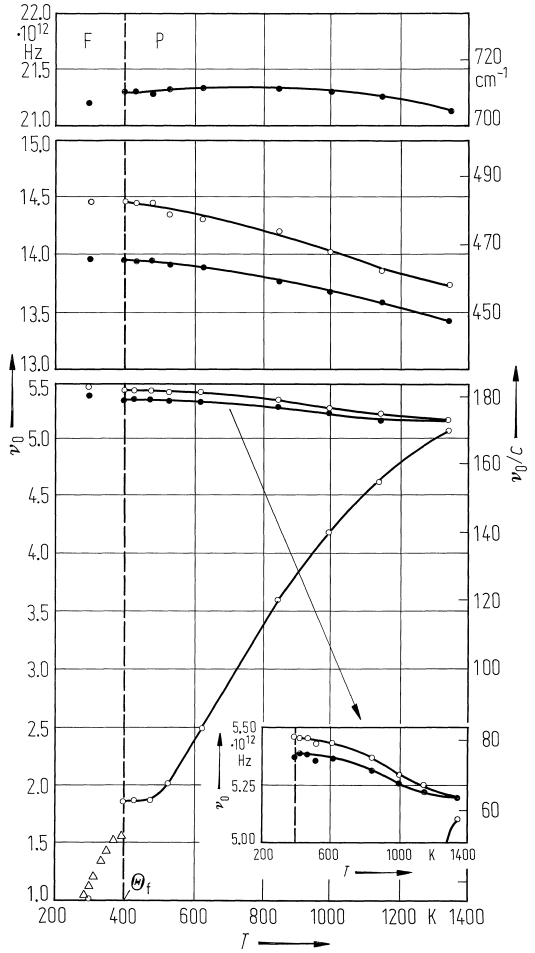

Fig. 1A-10-110. $BaTiO_3$. ν_0 vs. T [80Lus]. ν_0: frequencies of E modes below Θ_f and F_{1u} modes above Θ_f. Infrared measurement. Open circles: TO modes. Full circles: LO modes. Open triangles: Raman data taken from [77Sca].

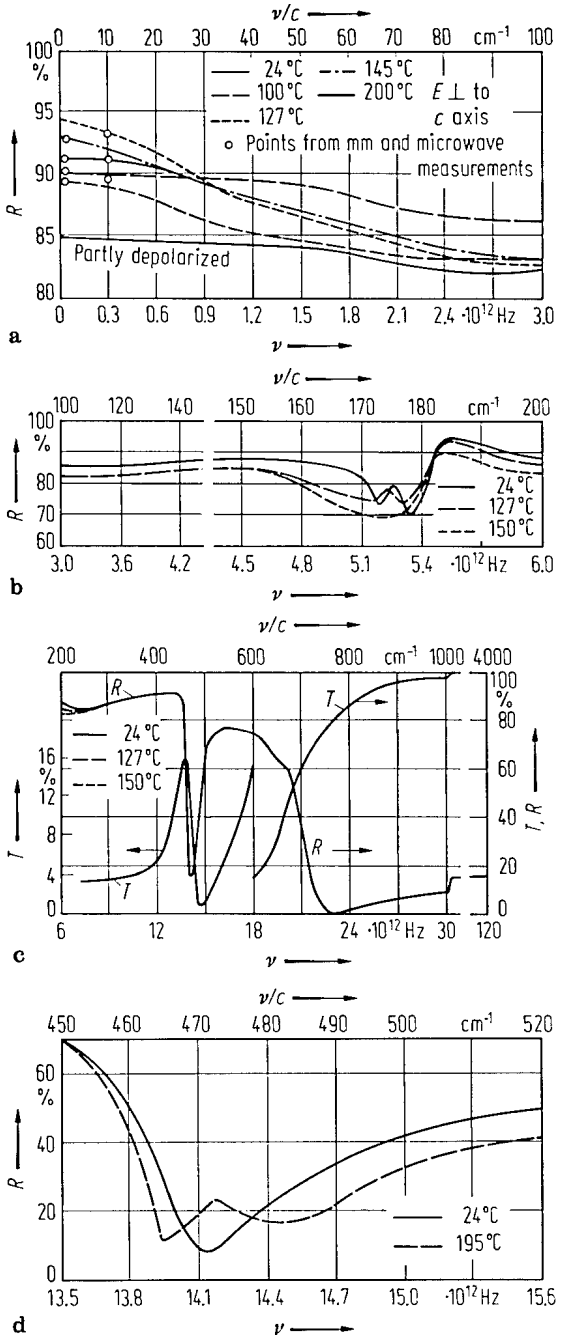

Fig. 1A-10-111. $BaTiO_3$. *R*, *T* vs. ν [64Bal]. *R:* reflectivity. *T:* transmission. Note change of scale at $\nu = 4.2 \cdot 10^{12}$ Hz in **(b)**.

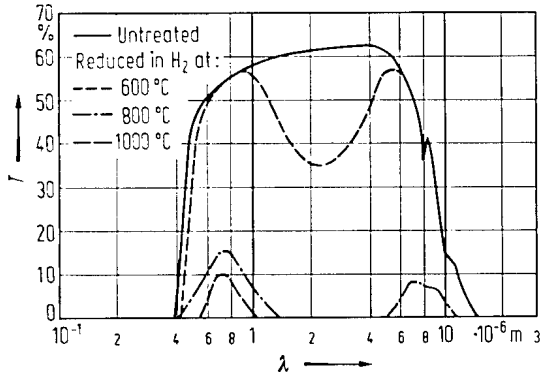

Fig. 1A-10-112. $BaTiO_3$. *T* vs. λ [64Ike]. *T:* transmission for the infrared radiation.

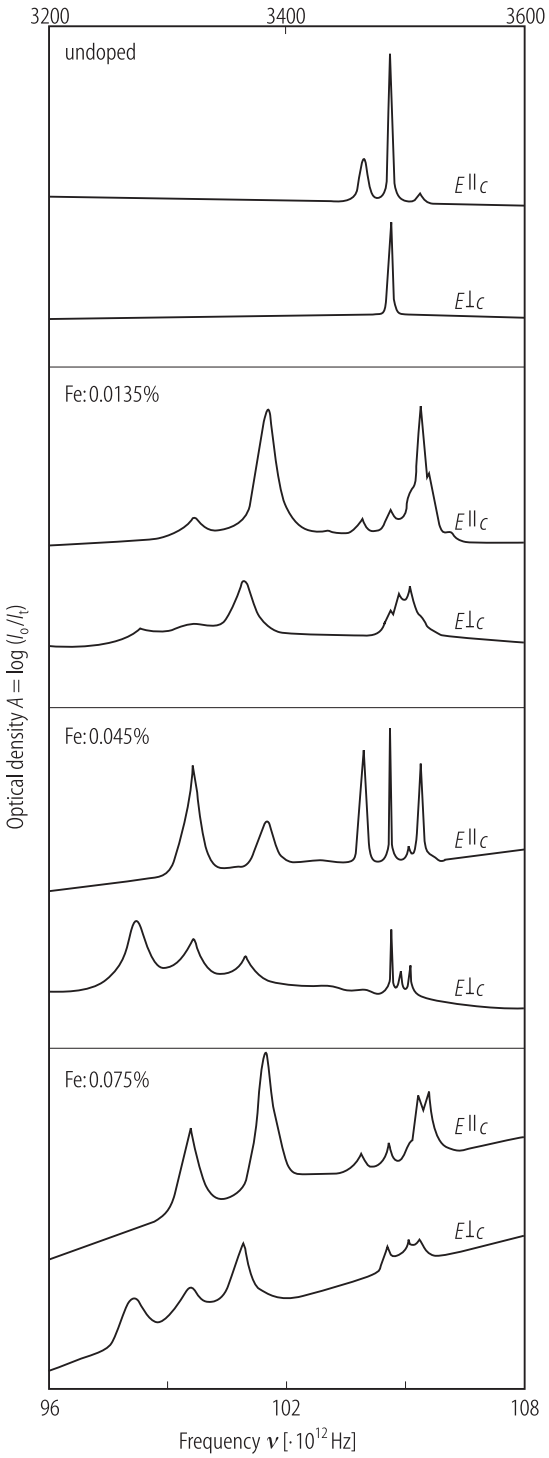

Fig. 1A-10-113. $BaTiO_3$ (Fe doped). Infrared absorption spectra due to OH vibration [89Jov]. *A*: optical density ($A = \log_{10} I_0/I_t$; I_0: intensity of incident light, I_t: intensity of transmitted light). Parameter: Fe concentration. *T* = RT.

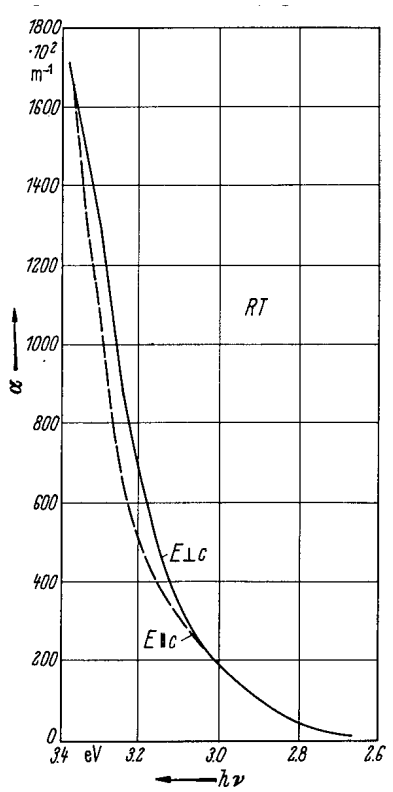

Fig. 1A-10-114. $BaTiO_3$. α vs. $h\nu$ [59Cas]. α: optical absorption coefficient. Polarized light.

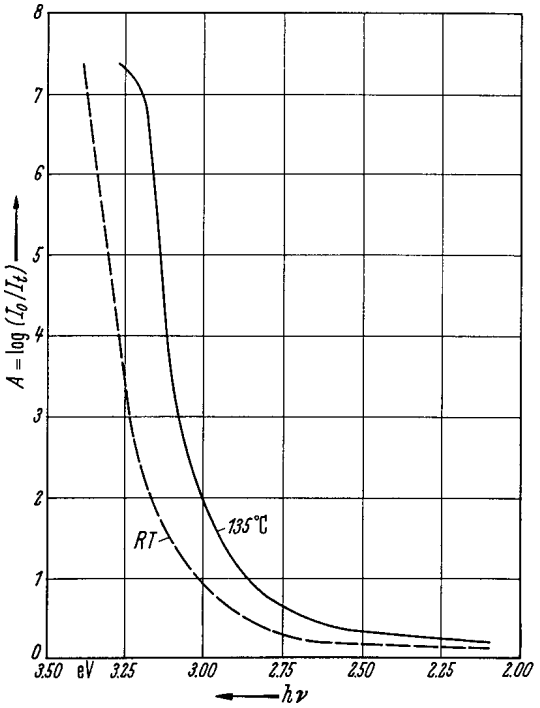

Fig. 1A-10-115. $BaTiO_3$. A vs. $h\nu$ [59Cas]. A: optical density ($A = \log_{10} I_0/I_t$; I_0: intensity of incident light, I_t: intensity of transmitted light). Unpolarized light.

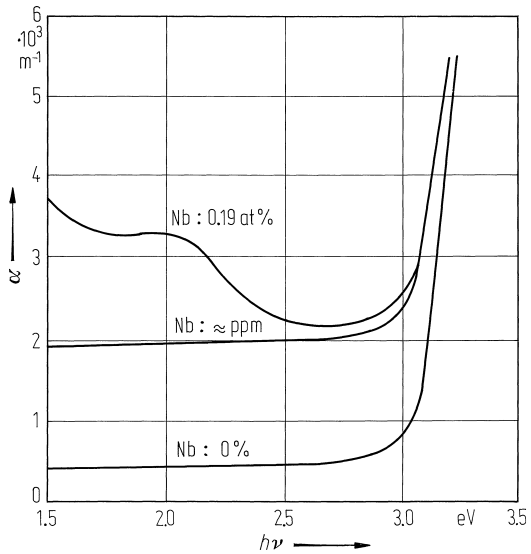

Fig. 1A-10-116. $BaTiO_3$ (Nb doped). α vs. $h\nu$ at RT [81Mor]. α: optical absorption coefficient. Parameter: Nb concentration. The crystal was grown by a pulling method.

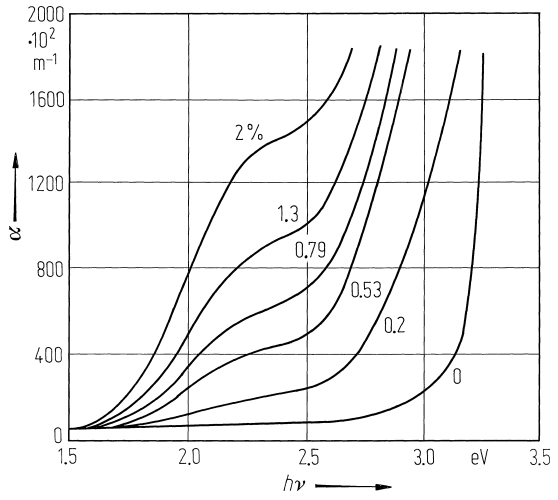

Fig. 1A-10-117. $BaTiO_3$ (Co doped). α vs. $h\nu$ at RT [83Mic]. α: optical absorption coefficient. Parameter: Co concentration. The crystal was grown by the KF flux method.

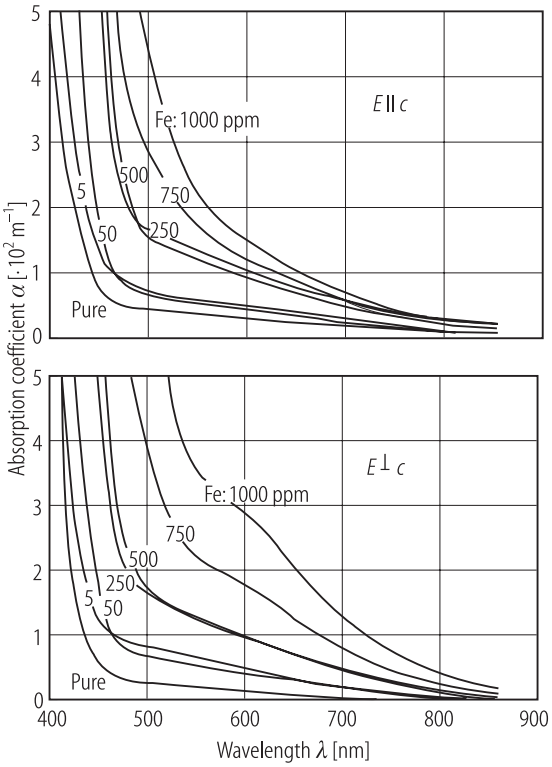

Fig. 1A-10-118. $BaTiO_3$ (Fe doped). α vs. λ at RT [88Sch2]. α: optical absorption coefficient. Polarized light: $\boldsymbol{E} \perp \boldsymbol{c}$ and $\boldsymbol{E} \parallel \boldsymbol{c}$. Parameter: Fe concentration (with respect to Fe/Ti ratio in the melt). The crystal was grown by the top-seeded solution growth method.

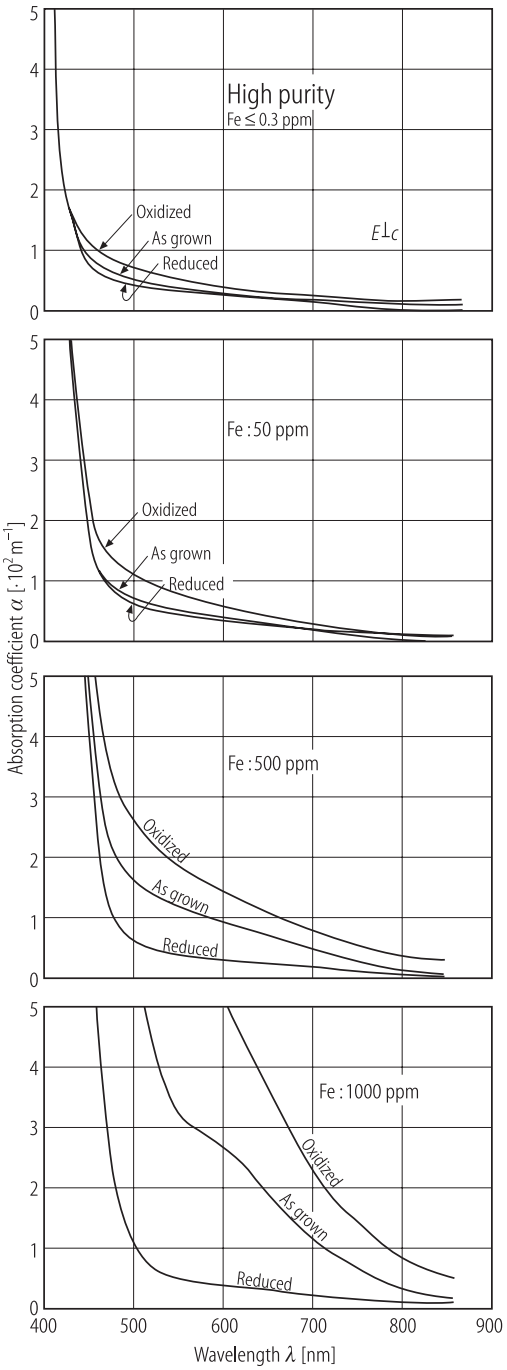

Fig. 1A-10-119. $BaTiO_3$ (Fe doped). α vs. λ at RT [88Sch2]. α: optical absorption coefficient. Polarized light: ***E*** perpendicular to the *c*-axis. Parameter: Fe concentration (with respect to Fe/Ti ratio in the melt). The crystal was grown by the top-seeded solution growth method. Oxidation was done at oxygen partial pressure $p_{O_2} = 10^5$ Pa and 800 °C. Reduction was done at $p_{O_2} = 10$ Pa and 800 °C.